Using Satellite Atmospheric Infrared Sounder (AIRS) and a Ground-based Global Positioning Satellite (GPS) Network to Validate the Precipitable Water Vapor in Global Climate Models (GCMs) and Numerical Weather Prediction (NWP) Regional Reanalysis

Jacola A. Roman, Robert O. Knuteson, Steven A. Ackerman, David C. Tobin, William L. Smith, and Henry E. Revercomb,

University of Wisconsin-Madison Space Science and Engineering Center (SSEC)
Cooperative Institute for Meteorological Satellite Studies (CIMSS)

1. INTRODUCTION

The Intergovernmental Panel on Climate Change (IPCC et al. 2007) fourth assessment concluded that the warming of the climate system is "unequivocal". There is evidence that water vapor amounts also increase with increasing global temperatures and saturation vapor pressure in the troposphere (Trenberth et al. 2005; Soden et al. 2005). Water vapor is an important greenhouse gas and is responsible for the dominant feedback in the climate system (Trenbert et al. 2007). Climate Models (GCMs) provide a way to predict the increase in the atmosphere's total water vapor content and feedback. Validation of the of the GCM's accuracy at predicting the PWV is required to provide confidence in the results.

We will try to assess the ability of the GCMs to predict the PWV, by comparing the simulated data to observations from 2000-2010. Four models used in the IPCC fourth assessment will be compared to ground based GPS, radiosonde observations, and satellite observations, as well as the North American Regional Reanalysis (NARR). Regional PWV trends, seasonal 5-year PWV means, and mixing ratio profiles will be analyzed.

2. DATA

This study makes use of GPS PWV observations from the SuomiNet network and the NOAA GPS-Met receivers installed at the NOAA Profiler Network (NPN) sites. SuomiNet is an international network of GPS receivers that provides 30-minute PWV measurements and is managed by the University Corporation for Atmospheric Research (UCAR). GPS-Met Observing Systems was created to develop and validate techniques for measuring PWV using ground based GPS receivers. GPS-Met data also provides 30-munute averaged PWV measurements. This GPS data was obtained through the Atmospheric Radiation Measurement Climate Research Facility (ARM) data archive (URL: http://www.arm.gov/data/vaps/suomigps).

Each GPS file contains a list of station names, numbers latitude, longitude, and elevation. For each station, measurements for PWV, surface relative humidity, surface pressure, and surface temperature are available starting June 7th 2001 for the SuomiNet data and January 1st 1996 for the NPN data. Figure 1 shows the locations of the SuomiNet and NPN GPS stations.

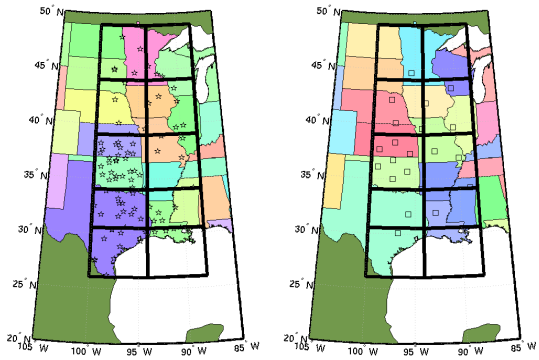

Figure 1. GPS station location maps showing the UCAR SuomiNet (left panel) and NPN (right panel) networks used in this study.

AIRS data was obtained from the NASA data archive at http://disc.sci.gsfc.nasa.gov/AIRS. The L3 ascending node science team product provides global gridded (1 degree) monthly means at about 1:30 pm local time. Each file contained latitude, longitude, and PWV measurements for each gridded point.

Radiosonde data was also obtained through the DOE ARM data archive. Data was available starting October 2nd, 2004 at the ARM Southern Great Plains (SGP) central facility site, near Lamont, Oklahoma. Each file contains vertical profiles of mixing ratio launched at 10-minute intervals (URL: http://www.arm.gov/intruments/rl).

NARR data used in this analysis was obtained through NOAA's National Operation Model Archive and Distribution System (NOMADS), and is available starting October 1978. The file contains three-hour averages for surface pressure, relative humidity, surface temperature, specific humidity, and PWV. (URL: http://nomads.ncdc.noaa.gov/data.php?name=access#narr_datasets).

GCM output was retrieved through the World Climate Research Programme (WRCP) Coupled Model Intercomparison Project Phase 3 (CMIP3) multi-model database. Each model output is available starting January 2000. For this study,

the Special Report on Emissions Scenarios (SRES) A2 run 1 simulation was chosen, which is described as: “a very heterogeneous world with continuously increasing global population and regionally oriented economic growth that is more fragmented and slower than in other storylines” (URL: http://www.ipcc-data.org/ar4/scenario-SRA2.html). The NCAR Community Climate System Model CCSM3, the Canadian Center for Climate Modeling and Analysis CGCM3.1 Model T47, the NASA Goddard Institute for Space Studies Model E20/Russell GISS, and the Parallel Climate Model (Version 1) PCM1 were selected for the study. Each file contained latitudes, longitudes, time, surface temperature, surface pressure, relative humidity profiles, temperature profiles, and PWV (URL: https://esgcet.llnl.gov:8443/home/public/HomePage.do).

3. Methodology

GPS observations, for both SuomiNet and NPN networks, were extracted for the desired region in the United States. PWV was averaged monthly for individual stations. Regional statistics were then calculated by first correcting for elevation, which accounts for the topographic variation within each study region. Latitudes and longitudes were determined for each region boundary, and then stations within this boundary were averaged together to create the mean, median, standard deviation, mean error, monthly mean climatology, and inter-annual variability for each region. Regional trends were calculated using the weighted least square fit for the trend with the weighting factor by month defined to be the inverse square root of the number of stations within each region. The uncertainty in the trend was calculated using the equations from Weatherhead et al. (1998). Figure 2 shows the trend for the Oklahoma/Kansas region from 2000 until 2010.

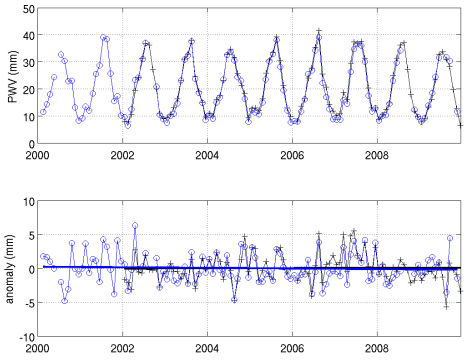

Figure 2. Monthly mean PWV (upper panel) and anomaly time series with trend fits (lower panel) in the Oklahoma/Kansas region for the arithmetic mean of Suominet (plus symbol) and NPN (circles) GPS stations.

GCM data as well as the satellite observations were already in the form of monthly averages. PWV was extracted for the same spatial and temporal span of the GPS data. From this, regional trends and uncertainties, for the GCMs, were calculated using the same methods applied to the GPS data. These trends were then directly compared to the GPS trends.

The satellite observations were validated at a specific site, the SGP CF in Lamont, OK. Here the AIRS L3 product and the AIRS L2 were compared to the ground-based GPS. This provided assessment of each product.

Another intercomparison method used was to calculate a seasonal eight-year mean and seasonal eight-year inter-annual variability for the two data sets. Four seasons were distinguished as follows: December/January/February (DJF), March/April/May (MAM), June/July/August (JJA), and September/October/November (SON). The regional averages were averaged over each season for each year, and then these seasonal averages were averaged over the eight years. Figure 3 shows the eight-year average for all regions for each model and the observations. In addition a three year season mean was calculated for the observations, both satellite and ground, and the models, but instead of looking at each region the latitudinal and longitudinal dependence was examined.

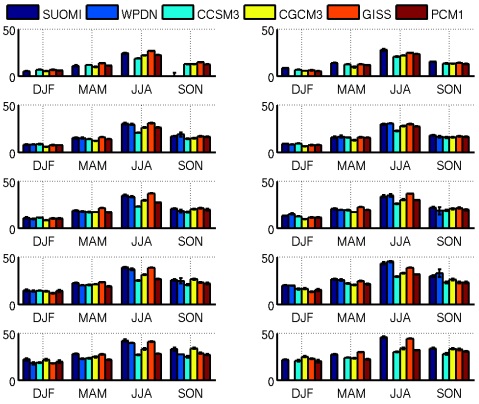

Figure 3. Seasonal PWV mean for all regions from 2000-2010

Profiles of mixing ratio, relative humidity, pressure, and temperature were extracted from both the GCMs and the radiosonde data at the SGP central facility site from 2005 to 2010. The GCM’s were interpolated to match the height scale of the radiosonde profiles. The difference at each level (GCM-Sonde) for each variable was calculated. Five year seasonal averages were computed using the same method applied to the surface data. The last comparison approach was

to calculate the average from 0 to 5km in the profile for each season and each variable and then differenced. This was also applied to the top of the profile (5km to 12km).

4. RESULTS

Results from ground-based GPS comparisons to GCMs can be found in Roman et al. 2012 (In Review). The predicted trend in total water vapor in the SRES A2 scenario for the period 2000-2100 for the OK/KS region is 0.0498+-0.0078mm/yr (CCSM3) and 0.0540+-0.0090 mm/yr (GISS). Trend results showed a large seasonal amplitude difference between GCM's, specifically between the GISS and CCSM3. A zero trend is predicted for the period 2000-2010 within a 95% confidence level for the GCMs. After elevation correction, the SuomiNet and NPN network observations showed a zero trend as well. Figure 4 shows the trends for all of the GCMs as well as the observations for the OK/KS region from 2000-2010 and the variability.

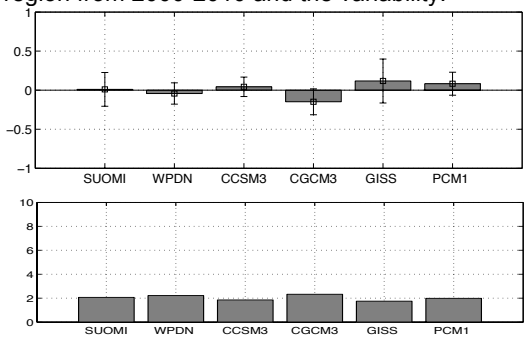

Figure 4. SuomiNet, NPN, and GCM trends (top panel) and standard deviation (bottom panel) for the Oklahoma/Kansas region from 2000-2010.

Since there was a null trend found from 2000-2010, the time to detect a trend of 0.05 mm/yr, the 100 year trend found in the GCMs, was examined. Figure 5 shows the number of years to detect a trend of this size for each region. There is a latitude dependence, the number of years decreases as you move northward.

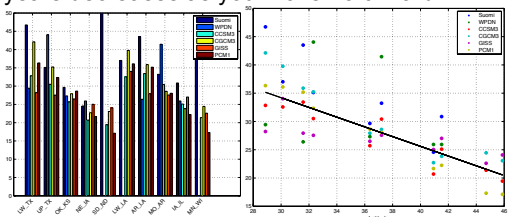

Figure 5. TTD a trend of 0.05 mm/yr for each region (left panel). The same information is presented again but showing the latitude dependence (right panel).

PWV biases occurred in the U.S. Great Plains for the GCMs. Seasonal variations in the PWV bias were observed versus GPS with the largest disagreements occurring in the northern hemisphere during summer. There was a consistent PWV bias within each model for the 10 regions studied. During wintertime there is a general agreement among the models for the OK/KS region, while during summer only the GISS model agreed with the GPS observations. Figure 6 shows the PWV mean for the OK/KS region, the GCM-GPS PWV difference, and the GCM fractional error relative to GPS PWV observations.

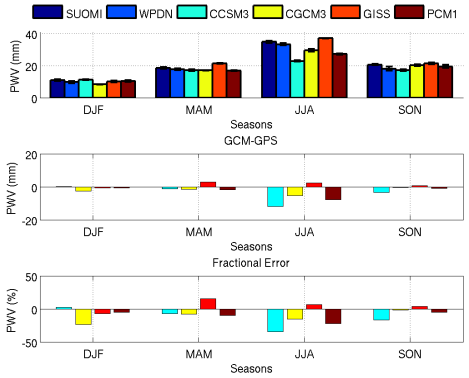

Figure 6. (upper) PWV mean (2000-2010) for the Oklahoma/Kansas region with error bars representing the uncertainty in the mean estimate (k=1). (middle) GCM-GPS PWV difference. (lower) GCM fractional error relative to GPS PWV observations.

A comparison of the NARR and AIRS L3 to the GCMS showed that the GISS model captures the moisture influx observed from the Gulf of Mexico in summer. Also, the GISS model is the only model that captures that enhancement of PWV over the Baja Peninsula. Figure 7 shows map plots of the GCM, AIRS, and NARR PWV for the month of August 2006.

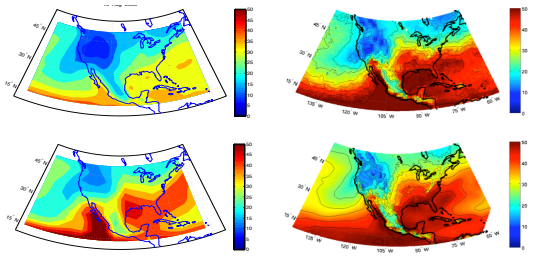

Figure 7. Map plots of CCSM3 (upper left), and GISS (bottom left) compared to the AIRS L3 (upper right) and NARR (bottom right) for August 2006.

Comparison of mixing ratio, relative humidity, and temperature profiles of the GCMs to the radisondes from 2005-2010 at the ARM SGP site confirmed the dry bias in the lower troposphere and indicated a moist bias in the upper

troposphere during the summer. The GISS model is the best at approximating the observations in the summer for the lower troposphere. Figure 8 shows profiles for models and radisondes at the SGP site for mixing ratio.

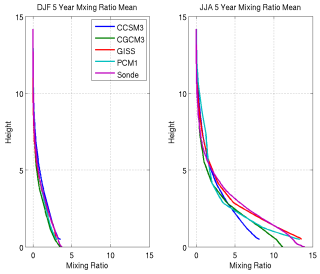

Figure 8. Mean GCM and ARM SGP radiosonde profiles for winter (DJF) and summer (JJA) over the period 2005-2010 for mixing ratio.

Large model-to-model variations in the lowest 5km for mixing ratio. The CCSM3 model is moist relative to the sonde observations above 5km. Figure 9 shows the GCM layered difference from the monthly mean radiosonde profile at the ARM SGP site for mixing ratio from 0 to 5 km and 5km to TOA.

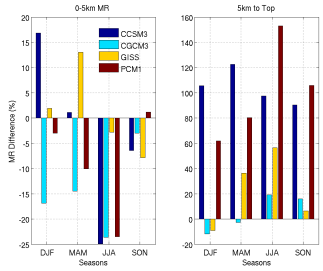

Figure 9. GCM profile errors (Model-Sonde) by season relative to radisondes for mixing ratio at the ARM SGP site for the layer averages 0-5 km (left panels) and 5-12 km (right panels).

Examining the northern hemisphere PWV, the ground-based GPS and AIRS L3 confirm the wintertime model PWV and the enhancement of PWV seen in the GISS during winter. Figure 10 shows the longitude average of 100 W to 94 W for all models and observations from 0 to 90 N for winter and summer.

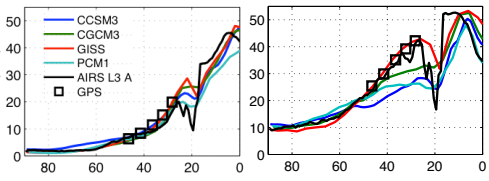

Figure 10. GCMs three year seasonal PWV compared to ground-based and satellite observations for winter (right) and summer (left). The longitude average was from 100 W to 94 W

Averaging from 32 N to 37 N and comparing the model PWV to the observations assessed the longitude dependence. An enhancement of PWV around 0 to 20 E, North Africa and the Mediterranean Sea, was shown in the GISS model during summer. This inter-model difference is very similar to the difference in the Great Plains and Midwest region. The AIRS L3 validates this new region as shown in figure 11.

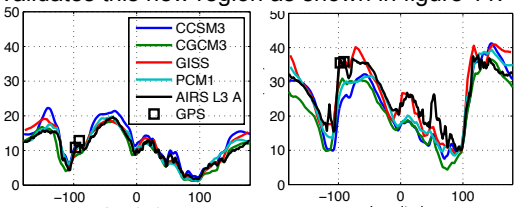

Figure 11. Three year seasonal mean PWV winter (left) and summer (right), shown for GCMs, ground-based GPS and AIRS L3 for a latitude average from 32 N to 37 N.

Expanding to the southern hemisphere, figure 12 shows initial results using AMSR-E and AIRS as the observational data. Again, looking at a three-year seasonal mean averaged from 87 W to 100 W, the latitude dependence indicates additional regions where inter-model differences are large for both winter and summer. This is especially pronounced at 0 to 20 S.

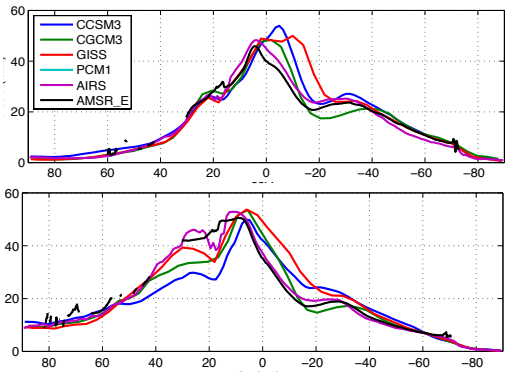

Figure 12. Three year seasonal mean PWV winter (top) and summer (bottom), showing GCMs, AMSR-E, and AIRS averaged from 87 W to 100 W.

5. CONCLUSIONS

The U.S. Great Plains and Midwest regions used in this study highlight the difference among the GCMs in their seasonal representation of the PWV and in the vertical distribution of moisture within the models. Elevation corrected GPS PWV trends are consistent with the zero trend found in the GCM data from 2000-2010. The GISS model best simulates the observations. Northward moisture flux from the Gulf of Mexico in the summer season represents the largest

variation from model to model. Vertical profiles of relative humidity, specific humidity, and temperature confirm that the GISS model most accurately represented the summer time specific humidity, although it contains biases above 5km, which are similar to other models. The GISS model in other regions, for example North Africa and the Mediterannean Sea, shows significant enhancement of PWV compared to other models, which is validated by the AIRS L3. In addition, other regions have been mentioned, 0 to 20 S, where large inter-model differences are prominent and in which none of the models match the AIRS and AMSR-E observations.

Acknowledgment

The data sets used in this analysis were obtained from ARM, the program sponsored by the U.S. Department of Energy, Office of Science, Office of Biological and Environmental Research, Climate and Environmental Sciences Division. This research also uses data provided by the Community Climate System Model project (www.ccsm.ucar.edu), supported by the Directorate for Geosciences of the National Science Foundation and the Office of Biological and Environmental Research of the U.S. Department of Energy. This work was supported under JPSS NOAA grant NA10NES4400013 and CLARREO NASA grant NNX08AP44G.

References

Bevis M., S. Businger, T.A. Herring, C. Rocken, R.A. Anthes and R.H. Ware, 1992. GPS Meteorology: Remote Sensing of Atmospheric Water Vapor Using the Global Positioning System, Journal of Geophys. Research, Vol. 97, No. D14, pp 787 - 801.

IPCC, Alley, R., Berntsen, T., Bindoff, N. L., et al. (2007), Climate change 2007: The physical basis – Summary for policy makers, Contribution of working group I to the Fourth Assessment Report of the Intergovernmental Panel on Climate Change (IPCC), IPCC web page (http://www.ipcc.ch/SPM2feb07.pdf), 2007.

Roman, J.A., Knuteson, R.O., Ackerman, S.A., et al. (2012), Validation of Regional Global Climate Model (GCM) Water Vapor Bias and Trends Using Precipitable Water Vapor (PWV) Observations from a Network of Global Positioning Satellite (GPS) Receivers in the U.S. Great Plains and Midwest. Journal of Climate (In Review).

Soden, B. J., D. L. Jackson, V. Ramaswamy, D. Schwarzkopf, and X. Huang, 2005: The radiative signature of upper tropospheric moistening. Science, 310, 841–844.

Trenberth, Kevin E., Lesley Smith, Taotao Qian, Aiguo Dai, John Fasullo, 2007: Estimates of the Global Water Budget and Its Annual Cycle Using Observational and Model Data, Journal of Hydrometeorology 2007 8:4, 758-769

Trenberth, K. E., J. Fasullo, and L. Smith (2005), Trends and variability in column-integrated atmospheric water vapor, Clim. Dyn., 24, 741–758.

Wolfe, D. and S.I.Gutman, 2000: Developing an operational, surface-based, GPS, water vapor observing system for NOAA: Network design and results. Journal of Atmospheric and Oceanic Technology, 17, 426-440.